



Short communication

Isolation, spectroscopic characterization, X-ray, theoretical studies as well as *in vitro* cytotoxicity of Samarcandin

Salar Hafez Ghoran^{a,*}, Vahideh Atabaki^b, Esmaeil Babaei^c, Seyed Reza Olfatkah^a, Michal Dusek^d, Vaclav Eigler^d, Alireza Soltani^e, Aliakbar Dehno Khalaji^{b,*}

^a Young Researchers and Elite Club, Maragheh Branch, Islamic Azad University, Maragheh, Iran

^b Department of Chemistry, Faculty of Sciences, Golestan University, Gorgan, Iran

^c Department of Animal Biology, School of Natural Sciences, University of Tabriz, Tabriz, Iran

^d Institute of Physics AS CR, v.v.i., Na Slovance 2, 182 21 Prague 8, Czech Republic

^e Joints, Bones and Connective Tissue Research Centre, Golestan University of Medical Science, Gorgan, Iran

ARTICLE INFO

Article history:

Received 27 January 2016

Revised 12 March 2016

Accepted 14 March 2016

Available online 15 March 2016

Keywords:

Cytotoxicity

NMR

Sesquiterpene coumarin

Theoretical study

TD-DFT

X-ray

ABSTRACT

Samarcandin **1**, a natural sesquiterpene-coumarin, was isolated as well as elucidated from *F. assa-foetida* which has significant effect in Iranian traditional medicine because of its medicinal attitudes. The crystal structure of samarcandin was determined by single-crystal X-ray structure analysis. It is orthorhombic, with unit cell parameters $a = 10.8204$ (5) Å, $b = 12.9894$ (7) Å, $c = 15.2467$ (9) Å, $V = 2142.9$ (2) Å³, space group $P2_12_12_1$ and four symmetry equivalent molecules in the unit cell. Samarcandin was isolated in order to study for its theoretical studies as well as its cellular toxicity as anti-cancer drug against two cancerous cells. In comparison with controls, our microscopic and MTT assay data showed that samarcandin suppresses cancer cell proliferation in a dose-dependent manner with $IC_{50} = 11$ μM and 13 for AGS and WEHI-164 cell lines, respectively. Density functional theory (DFT) and time-dependent density functional theory (TD-DFT) of the structure was computed by three functional methods and 6-311++G** standard basis set. The optimized molecular geometry and theoretical analysis agree closely to that obtained from the single crystal X-ray crystallography. To sum up, the good correlations between experimental and theoretical studies by UV, NMR, and IR spectra were found.

© 2016 Elsevier Inc. All rights reserved.

1. Introduction

Sesquiterpene-coumarins are a large group of natural compounds whose structures are based on a C₁₅ terpene moiety linked through an ether linkage with the 7-hydroxy group. The origin of sesquiterpene-coumarins are the families Apiaceae (Umbelliferae), Asteraceae (Compositae) and Rutaceae. They find in the genera such as *Ferula*, *Heptapetra*, *Heraclum*, *Peucedanum*, *Angelica* (Apiaceae), *Artemisia* (Asteraceae) and *Haplophyllum* (Routaceae) [1].

Abbreviations: DFT, density functional theory; DMEM, Dulbecco's modified Eagle's medium; FBS, fetal bovine serum; FT-IR, Fourier transform infrared spectroscopy; GIAO, gauge included atomic orbital; HOMO, highest occupied molecular orbital; LUMO, lowest unoccupied molecular orbital; TD-DFT, time-dependent density functional theory; TLC, thin layer chromatography; NMR, nuclear magnetic resonance; MTT, 3-[4,5-dimethylthiazol-2-yl] 2,5-phenyltetrazolium bromide; UV-Vis, ultraviolet-visible.

* Corresponding authors.

E-mail addresses: S_Hafezghoran@yahoo.com, S.Hafezghoran@gu.ac.ir (S.H. Ghoran), Alidkhalaji@yahoo.com (A.D. Khalaji).

Among these genera, an array of different sesquiterpene-coumarins have been reported from *Ferula* species. Thus, there is a substantial attention to the chemistry and pharmacology of plants belonging to the *Ferula* species which are traditionally used for the treatment of various diseases such as asthma, epilepsy, stomach-ache, flatulence, intestinal parasites, weak digestion and influenza [2–5]. Recent biological studies on oleo-gum-resin of *Ferula* species have markedly shown as antioxidant [6], anticonvulsant [7], antibacterial [8], antiviral [5], antifungal [9–11], cancer chemopreventive [12,13], anti-diabetic [14], antispasmodic, hypotensive [15], as well as molluscicidal [16]. As far as a huge number of cyclic sesquiterpene-coumarins, including compounds feselol, coladin, coladonin, isosamarcandin and mogoltacin, isolated from *F. gumosa*, *F. tunetana* and *F. Badrakema* displayed various effects against several human cancerous cell lines [17–19], the purpose of the present study is to provide theoretical studies as well as cellular toxicity of samarcandin, an isolated sesquiterpene-coumarin from *F. assa-foetida*, based on its cytotoxic characteristics on cancerous AGS (Stomach for human) and

WEHI-164 (Skin from mouse fibrosarcoma) cells. In addition, it is worth to mention that samarcandin (CCDC No. 1015760, C₂₄H₃₂O₅, refer to Fig. 1) was initially isolated from ethereal extract of *F. samarcandica* Kor. and its infrared (IR) as well as UV spectra were also studied [20,21]. Subsequently, its three-dimensional structure along with absolute configuration was determined with X-ray crystallography by Nasirov et al. [22]. However, theoretical studies and cytotoxic activity on samarcandin has, to date, not been carried out. Hence, in the present research, the chemical structure of samarcandin **1** was elucidated by experimental NMR, IR, UV as well as theoretical methodology using by B3LYP [23–28] functional and 6-311++G** standard basis set.

2. Experimental

2.1. Plant material

Oleo-gum-resin obtained from *Ferula assa-foetida* L. root were collected from hills of Tangesorkh from Yasouj of Kohgiluyeh and Boyer-Ahmad province, Iran, in May 2014. Tangesorkh is a swampy area where *F. assa-foetida*'s is collected for the export outside Iran. The plant was identified by Agriculture and Natural Recourses Research Centre, Yasouj, Iran, and a voucher specimen (No. 4412) was deposited in the Herbarium of the same institute.

2.2. Instruments and materials

All reagents and solvents for analysis were commercially available and used as received without further purifications. IR spectra were recorded on a Perkin-Elmer FT-IR instrument, using KBr disks, over the range 400–4000 cm⁻¹. The UV spectra in CHCl₃ solvent were measured by Shimadzo spectrophotometer. ¹H and ¹³C NMR experiments were carried out on a Bruker AV-400 NMR spectrometer with TMS as an internal standard. Column chromatography was performed on 230–400 mesh silica gel (Merck, Germany). TLC was performed on Merck F₂₅₄ silica gel plates (10 × 10 cm) (Merck, Germany). Spots on TLC were detected by UV₂₅₄. X-ray diffraction experiments were carried out on a Gemini four circle kappa diffractometer of Agilent Technologies using mirrors-collimated Mo K α radiation ($\lambda = 0.7107 \text{ \AA}$).

2.3. Extraction and isolation

Oleo-gum-resin obtained from *F. assa-foetida* L. (100 g) was extracted with Et₂O (250 mL) at reflux for 24 h. The extract was concentrated under reduced pressure to obtain a residue (45 g). The Et₂O extract (7 g) was separated by chromatography using a silica gel column and eluted with a gradient of n-hexane:EtOAc (9.7:0.3, 9:1, 8:2, 7:3, 6:4, 5:5, 3:7 and 0:10 (v/v)) to give eight fractions (F_A–F_H). Fraction F_{E1} (420 mg, n-hexane:EtOAc, 6:4) was purified by recrystallization by using n-hexane:EtOAc to obtain the samarcandin as white crystals (61 mg, with R_f: 0.72 for n-hexane:EtOAc, 96:4). It was shown by only one spot on TLC paper under UV₂₅₄ and there was no need for further purification.

2.4. X-ray crystal structure analysis of samarcandin

A single crystal of the dimensions 0.66 mm × 0.52 mm × 0.40 mm for samarcandin was chosen for the X-ray diffraction study. Crystallographic measurements were carried out at 120 K with a four circle CCD diffractometer, Gemini of Oxford Diffraction, Ltd., with graphite-monochromated Mo K α radiation ($\lambda = 0.7107 \text{ \AA}$), using Mo-Enhance fiber optics collimator and the CCD detector Atlas. The crystal structure of samarcandin was solved by program Superflip [29] and refined with Jana2006

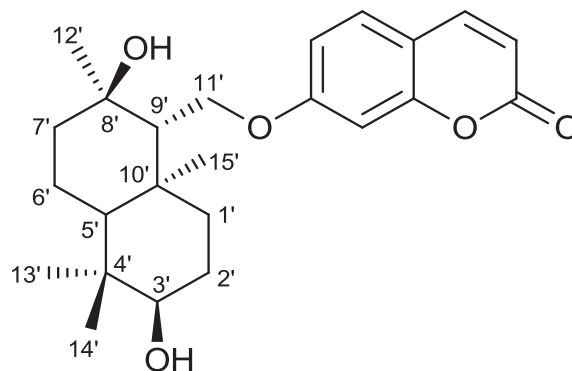


Fig. 1. Chemical structure of Samarcandin isolated from *F. assa-foetida*.

program package [30] by the full-matrix least-squares technique on F2 [29]. The molecular structure plots were prepared by ORTEP-III. All hydrogen atoms present in the structure model were discernible in difference Fourier maps and could be refined to reasonable geometry. According to common practice H atoms bonded to C were kept in ideal positions with C–H = 0.96 Å while positions of H atom bonded to O were refined freely. In both cases Uiso (H) was set to 1.2Ueq (C,O). All non-hydrogen atoms were refined using harmonic refinement. The hydrogen atoms of partially occupied water molecule could not be found in difference Fourier map and therefore they are absent in the structure model.

2.5. Computational procedures

The geometry optimization of samarcandin was studied by using density functional theory (DFT) calculations in combination with the B3LYP, BLYP and B3PW91 methods and 6-311++G** standard basis set [24,31,32]. All calculations were carried out with the Gaussian 98 program [28]. The selected bond lengths, angles and torsion angles of samarcandin are shown in Table 3. After full optimization, the vibrational calculation was studied by B3LYP method. The nuclear magnetic resonance NMR in our calculation (B3LYP method) was verified by the gauge included atomic orbital approach (GIAO) method [33,34]. We also performed Time-dependent density functional theory (TD-DFT) calculations in gas phase by B3LYP/6-311++G** level of theory. The harmonic frequency calculation at the same levels is studied [35,36].

2.6. Measurements of cell growth inhibition

Details of measuring cell growth inhibition are explained elsewhere [37]. Two cell lines including WEHI-164 and AGS (both from Pasteur Institute, Tehran, Iran) were grown in Dulbecco's modified Eagle's medium (DMEM; GIBCO®, USA) containing 10% fetal bovine serum (FBS; GIBCO®, USA) at 37 °C in a humidified atmosphere of 5% CO₂. Cell viability was measured by MTT (3-[4,5-dimethylthiazol-2-yl] 2,5-iphenyltetrazolium bromide) assay according to the manufacturer's instructions (Sigma-Aldrich, USA). Briefly, cancerous AGS and WEHI-164 cells and normal fibroblasts were seeded onto 96-well plates and allowed to adhere and grow overnight in 200 µl DMEM medium. The cells were then incubated with fresh medium containing serial concentrations (0–200 µM) of samarcandin dissolved in 1% DMSO for 48 h. Dendrosomal curcumin as an anti-proliferative compound was also employed as positive control. Afterward, 20 µl of 5 mg/ml MTT was added to each well and incubated for additional 4 h at 37 °C followed by addition of 200 µl of DMSO [37]. The relative cell viability was determined at 540 nm by a 96-well plate reader (Biorad-USA) and the concentration at which cell growth was inhibited by

50% (IC₅₀) was determined by standard curve method [38]. Each experiment was carried out in triplicate wells and repeated at least three times from each other.

2.7. Study of morphological changes in treated cells

Based on our previous work, morphological changes of all cancer cell lines were studied under invert microscope (Nikon-Japan) during treatment. Briefly, cells treated with 10 μM of samarandin and their time-dependent changes evaluated within 24 h treatment; at 4, 8, 16 and 24 h. All experiments were carried out in triplicate cell culture plates and compared with non-treated cells.

3. Results and discussion

3.1. Spectroscopic characterization and theoretical studies

One crystalline sesquiterpene coumarin was isolated by column chromatography method in Et₂O extract. After recrystallization in methanol and chloroform as well as booming attained crystals, samarandin was utterly characterized by spectroscopy and comparison with the literature data (see Fig. 1).

The spectroscopic data of samarandin **1** showed strong similarities to those of Badrakemin. The ¹H NMR spectrum showed that an extra methyl singlet in compound **1**. It is noteworthy to note that in the ¹³C NMR spectra of Badrakemin, the signals of two olefinic carbons from (δ_C 107.6, CH₂, and 146.7, C) were replaced by a methyl group and a quaternary carbon at δ_C 21.9 and 70.7 in **1** [39]. The ¹H NMR spectra of samarandin exhibited resonances of five methine signals at δ_H 6.1 (1H, d, *J* = 9.1 Hz), 7.9 (1H, d, *J* = 9.1 Hz), 7.7 (1H, d, *J* = 8.8 Hz), 6.9 (1H, dd, *J* = 2.4, 8.8 Hz), and 7.0 (1H, d, *J* = 2.4 Hz) assigned to H₃, H₄, H₅, H₆, and H₈ of the coumarin moiety, respectively. The methylene protons - H_{11'a} as well as H_{11'b} - showed a different splitting than those reported in the literature with one of them appeared as double doublet signal at δ_H 4.33 (1H, dd, *J* = 10.3, 3.9 Hz), and with the second one appeared as a doublet signal at δ_H 4.10 (1H, dd, *J* = 10.3, 7 Hz), respectively. An additional oxygenated proton (H_{3'}) was found at δ_H 3.4 (brs). The four methyl signals at δ_H 1.07 (s), 0.71 (s), 0.80 (s), and 0.92 (s) ppm were assigned to H_{12'}, H_{13'}, H_{14'}, and H_{15'}, respectively. The ¹³C NMR spectrum (Table 1) showed signals for 24 carbons, which were assigned with the aid of DEPT spectra to four methyl, five methylene, eight methine, and seven quaternary carbons. Two carbon resonances at δ_C 73.5 (CH) as well as 70.7 (C) suggested the presence of oxygen-bearing sp³ carbons. The downfield signal at δ_C 161.8 ppm was assigned to the carbonyl carbon of the coumarin moiety (C₂) (see Table 1). In theoretical calculation, the ¹H NMR spectrum indicates that the values of H₃, H₄, H₅, H₆, and H₈ peaks are calculated to be 6.25, 7.94, 7.54, 6.89, and 7.16 ppm at the B3LYP/6-311++G** level of theory, respectively. Our calculations on ¹H NMR imply an acceptable agreement with the experimental values. The IR spectrum displayed the presence of hydroxyl (3432 cm⁻¹), α-pyrone ring (1680 cm⁻¹), aromatic ring (1589 cm⁻¹), aliphatic hydrogens (2925 cm⁻¹), and etheric oxygen (1102 cm⁻¹). These data suggested that compound samarandin can be derived from sesquiterpene and umbelliferone components [40]. The bonds between 1557 and 1684 cm⁻¹ are assigned to C–C stretching vibration [41]. The C=O stretching bond is observed at 1770 cm⁻¹ in IR calculations. The vibrational analysis of this structure was carried out over the basis of the characteristic vibrations methylene, hydroxyl, etheric oxygen, aliphatic hydrogens, and carbon aromatic ring modes. Theoretical calculations were done at the B3LYP method and 6-311++G** standard basis set. The value of the C–H stretching of the carbon aromatic ring occurs in the region 3196–3257 cm⁻¹. A band observed at 3490 cm⁻¹ in IR spectrum

Table 1
NMR spectroscopic data for Samarandin **1** (in CDCl₃).

Position	δ _H (J in Hz)	δ _C
1'a	1.54, td (13.4, 3)	32.35
1'b	1.20, dd (13.4, 8)	
2'a	1.79, brt (13.4, 3)	24.80
2'b	1.32, dd (13.4, 8)	
3'	3.41, broad signal	73.50
4'	–	36.99
5'	1.42, broad signal	47.79
6'a	1.28, broad signal	19.54
6'b	1.45, dd (11.9, 4)	
7'a	1.49, broad signal	43.97
7'b	1.72, dd (11.9, 4)	
8'	–	70.73
9'	1.62, d (6.8)	59.47
10'	–	37.40
11'a	4.33, dd (10.3, 3.9)	66.19
11'b	4.10, dd (10.3, 7)	
12'	1.07, s	21.94
13'	0.71, s	24.38
14'	0.80, s	28.68
15'	0.92, s	15.63
2	–	15.91
3	6.1, d (9.1)	112.00
4	7.9, d (9.1)	144.18
5	7.7, d (8.8)	129.25
6	6.9, dd (8.8, 2.4)	113.11
7	–	161.80
8	7.0, d (2.4)	101.16
9	–	155.51
10	–	111.88
3'-OH	4.20	–
8'-OH	4.51	–

is assigned to hydroxyl stretching. The C–H stretching vibration in α-pyrone ring occurs in the region 3022–3117 cm⁻¹. A peak appearing at 1113 cm⁻¹ is assigned as C–O (etheric oxygen) stretching vibration in IR spectrum. The UV spectrum of samarandin exhibited two peaks in 326 nm and 244 nm wavelengths, which can be related to C=O of coumarin part (C₂) and double bonds of aromatic ring, respectively. The time-dependent density functional theory (TD-DFT) calculations were carried out by using B3LYP functional and 6-311++G** standard basis set [42,43]. At the present study the TD-DFT is computed by excited states oscillator strengths for samarandin within the gas phase. We observed the three optical transitions for this compound, however, only two terms contribute significantly to the oscillator strength: HOMO → LUMO (H → L), with 95% of the 0.4665 oscillator strength and transition energy of 4.05 eV; and H-1 → LUMO with 84% of the 0.0049 oscillator strength and transition energy of 4.33 eV. The theoretical result reveals that the first excitation energy maximum is predicted at λ_{max} = 316 nm with the 0.4665 oscillator strength that is in excellent agreement with experimental measurement (λ_{max} = 326 nm). In the theoretical results, the second excitation energy minimum is observed at λ_{max} = 266 nm, while the experimental data indicates the signal peak in the region of 244 nm.

3.2. Crystal structure of samarandin

The crystal structure of samarandin with the atom-numbering scheme is presented in Fig. 2. Crystallographic data, details of the data collection and structure solution and refinements are listed in Table 2, while the selected bond distances, angles and torsion angles are present in Table 3. The asymmetric unit consists of one molecule of samarandin and a fraction 0.094(4) of the lattice water. The C₄–O₅ bond length of 1.2074 (19) Å matches the value for double bond C=O, while the bonds C₄–O₃ (1.3729 (18)), C₂–O₃ (1.3823 (16)), C₁₁–O₁₂ (1.3553 (16)), C₁₃–O₁₂ (1.4439 (17)), C₁₅–O₁₇ (1.4410 (17)), and C₂₄–O₂₅ (1.4282 (18) Å) correspond

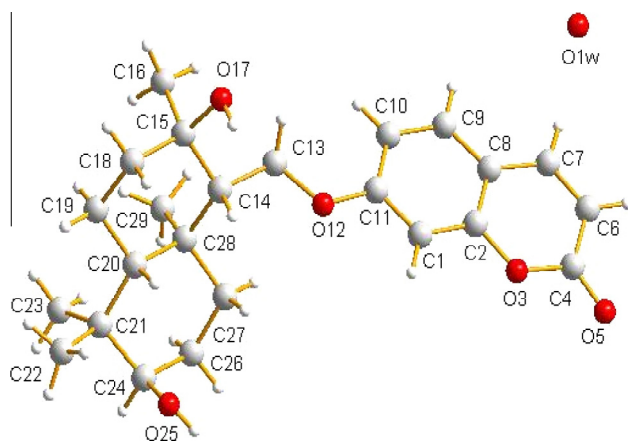


Fig. 2. An ORTEP view of Samarcandin.

Table 2
Crystallographic data of Samarcandin.

Empirical formula	C ₂₄ H ₃₂ O ₅
Formula weight	402
Crystal system	Orthorhombic
Space group	P2 ₁ 2 ₁ 2 ₁
Unit cell dimensions (Å)	a = 10.8204 (5) b = 12.9894 (7) c = 15.2467 (9)
Volume (Å ³)	2142.9 (2)
Z (atoms/unit cell)	4
D _{calc} /g cm ⁻³	1.24595
T (K)	120.1 (5)
μ (mm ⁻¹)	0.09
F (0 0 0)	867.0
Crystal size (mm)	0.66 × 0.52 × 0.40
S	1.31
R[F ² > 3σ(F ²)]	0.033
wR(F ²)	0.089
Δρ _{max}	0.14
Δρ _{min} (e Å ⁻³)	-0.11

to the value for single bonds C–O. The bond angles O₅–C₄–O₃ (116.57 (13)°) and O₅–C₄–C₆ (126.03 (15)°) in samarcandin are consistent with the sp² hybrid character of C₄, while the bond angles O₁₂–C₁₃–C₁₄ (107.73 (11)°) and C₁₃–C₁₄–C₁₅ (110.69 (11)°) in samarcandin are consistent with the sp³ hybrid character of C₁₃ and C₁₄, respectively. Crystallographic data (excluding structure factors) for the structure reported in this paper has been deposited with the Cambridge Crystallographic Centre, CCDC No. 1015760. Copies of the data could be obtained free of charge on application to The Director, CCDC, 12 Union Road, Cambridge CB2 1EZ, UK, fax: +44 1223 336 033, e-mail: deposit@ccdc.cam.ac.uk or <http://www.ccdc.cam.ac.uk>.

3.3. Theoretical analyses

The electronic densities in the HOMO (highest occupied molecular orbital) and LUMO (lowest unoccupied molecular orbital) for samarcandin was studied at the B3LYP, BLYP, and B3PW91 methods. Our calculations showed that the energy levels of HOMO and LUMO are -6.34 and -1.99 eV (B3LYP), -5.43 and -2.55 eV (BLYP), and -6.38 and -2.00 eV (B3PW91), respectively. As shown in Fig. 3, the HOMO orbital of this molecule is primarily located on the coumarin skeleton, O₁₂ and C₁₃, while the LUMO orbital is situated on the coumarin skeleton and O₁₂. The HOMO–LUMO energy separation has been interpreted as an indicator of kinetic stability of the system [31,36]. The energy gap values of samarcandin is calculated to be 4.35, 4.38, 2.88 eV at the B3LYP, BLYP, and B3PW91

Table 3
Experimental selected bond distances, bond angles and dihedral angles of Samarcandin compared with its theoretical data.

	Experimental	Theoretical		
		B3LYP	B-LYP	B3PW91
C ₄ –O ₃	1.37 (18)	1.37	1.37	1.37
C ₄ –O ₅	1.21 (19)	1.20	1.20	1.21
C ₂ –O ₃	1.38 (16)	1.38	1.38	1.38
C ₁₁ –O ₁₂	1.36 (16)	1.36	1.37	1.35
O ₁₂ –C ₁₃	1.44 (17)	1.44	1.46	1.43
C ₁₃ –C ₁₄	1.53 (19)	1.54	1.57	1.53
C ₁₅ –C ₁₆	1.52 (2)	1.53	1.54	1.53
C ₁₅ –O ₁₇	1.44 (17)	1.45	1.47	1.44
C ₂₁ –C ₂₂	1.54 (2)	1.55	1.56	1.54
C ₂₁ –C ₂₃	1.53 (2)	1.54	1.56	1.54
C ₂₄ –O ₂₅	1.43 (18)	1.44	1.46	1.43
C ₂₈ –C ₂₉	1.54 (19)	1.55	1.56	1.54
O ₃ –C ₄ –O ₅	116.57 (13)	117.51	116.84	117.53
O ₅ –C ₄ –C ₆	126.03 (15)	126.47	127.46	126.36
C ₁ –C ₁₁ –O ₁₂	115.13 (12)	115.50	115.25	115.55
C ₁₀ –C ₁₁ –O ₁₂	124.41 (12)	124.33	124.52	124.27
C ₁₁ –O ₁₂ –C ₁₃	117.42 (10)	119.28	119.06	118.92
O ₁₂ –C ₁₃ –C ₁₄	107.73 (11)	108.31	108.14	108.39
C ₁₃ –C ₁₄ –C ₁₅	110.69 (11)	110.67	110.67	110.69
C ₁₃ –C ₁₄ –C ₂₈	114.74 (11)	115.37	115.46	115.23
C ₁₆ –C ₁₅ –O ₁₇	104.19 (11)	103.10	102.79	103.33
C ₂₂ –C ₂₁ –C ₂₃	107.20 (13)	106.74	106.71	106.84
C ₂₁ –C ₂₄ –O ₂₅	108.31 (11)	107.62	107.53	107.64
C ₂₁ –C ₂₄ –C ₂₆	112.59 (12)	113.10	113.26	112.86
O ₂₅ –C ₂₄ –C ₂₆	110.39 (11)	110.24	110.22	110.37
C ₁₄ –C ₂₈ –C ₂₀	106.27 (10)	106.21	106.17	106.19
C ₁₄ –C ₂₈ –C ₂₇	108.26 (10)	108.16	108.20	108.01
C ₁₄ –C ₂₈ –C ₂₉	111.63 (11)	111.71	111.63	111.73
C ₂₀ –C ₂₈ –C ₂₉	113.96 (11)	113.87	113.96	113.92
C ₂₇ –C ₂₈ –C ₂₉	108.80 (11)	108.62	108.68	108.73
C ₁ –C ₁₁ –O ₁₂ –C ₁₃	-174.13	-179.66	-179.83	-179.46
O ₅ –C ₄ –C ₆ –C ₇	175.38	179.81	179.78	179.80
C ₁₀ –C ₁₁ –O ₁₂ –C ₁₃	5.68	0.45	0.28	0.65
C ₁₁ –O ₁₂ –C ₁₃ –C ₁₄	178.90	178.14	177.93	178.71
O ₁₂ –C ₁₃ –C ₁₄ –C ₁₅	135.63	137.49	136.55	136.59
O ₁₂ –C ₁₃ –C ₁₄ –C ₂₈	-91.37	-88.71	-89.52	-89.64
C ₁₅ –C ₁₄ –C ₂₈ –C ₂₉	69.57	69.12	69.39	68.94
O ₁₇ –C ₁₅ –C ₁₈ –C ₁₉	-168.98	-167.44	-167.31	-167.84
C ₁₉ –C ₂₀ –C ₂₁ –C ₂₂	-59.54	-58.75	-58.80	-58.68
C ₂₂ –C ₂₁ –C ₂₄ –C ₂₆	-168.88	-170.46	-170.09	-170.85
C ₂₂ –C ₂₁ –C ₂₀ –C ₂₈	168.88	169.44	169.21	169.68
C ₂₃ –C ₂₁ –C ₂₀ –C ₂₈	-71.08	-70.54	-70.82	-70.17

methods, respectively. The calculated HOMO–LUMO plots and total electron density of samarcandin using 6-311++G** basis set are shown in Fig. 3. The molecular electrostatic potential (MEP) shows that oxygen atoms are negatively charged (red¹ color) while the hydrogen atoms of hydroxyl groups are positively charged (blue color) (see Fig. 3).

3.4. Cancer cell growth inhibition

To explore the biological activity of samarcandin against cancer cell proliferation, the *in vitro* cytotoxicity was performed by studying the cell morphology and MTT assay. The cytotoxicity of samarcandin, with dendrosomal curcumin as positive control, was studied in the following cancer cell lines: AGS (Human gastric carcinoma) and WEHI-164 (Skin from mouse fibrosarcoma). The IC₅₀ value represents the amount of drug needed to inhibit 50% of the cancer cell growth, and it was attained after 48 h of exposition. The results displayed that samarcandin affects significantly the viability of cancerous AGS and WEHI-164 cells with IC₅₀ values of 11 μM and 13 μM, respectively. In contrast, dendrosomal

¹ For interpretation of color in Fig. 3, the reader is referred to the web version of this article.

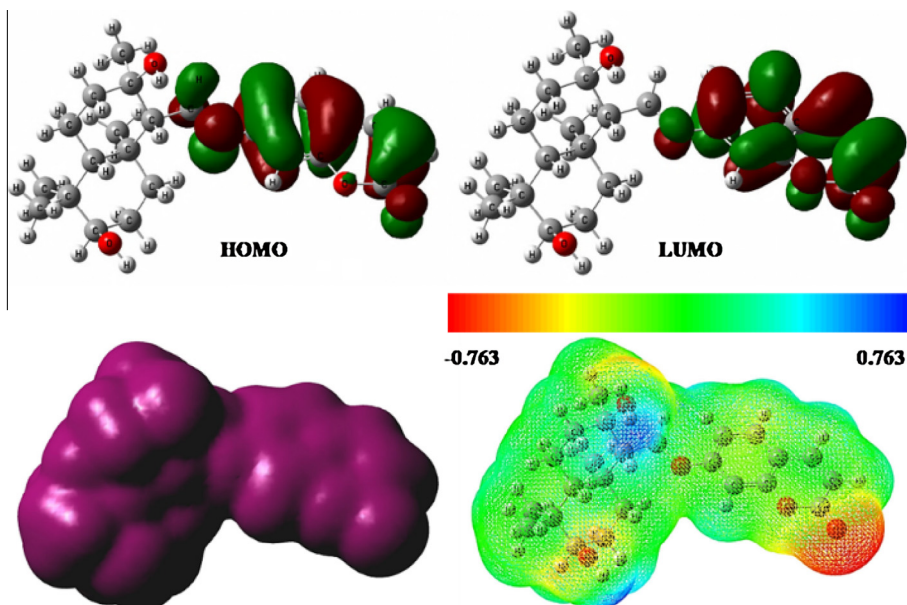
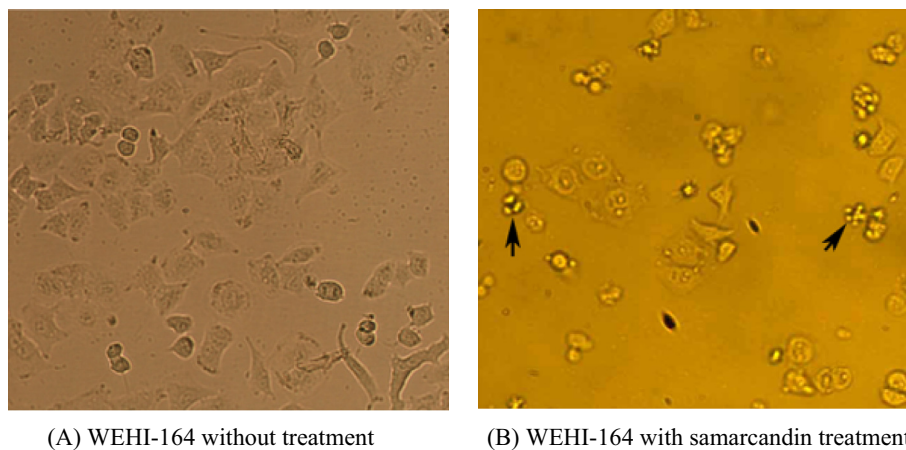


Fig. 3. Distribution patterns of frontier molecular orbitals for *Samarcandin* using B3PW91/6-311++G** basis set.



(A) WEHI-164 without treatment

(B) WEHI-164 with samarcandin treatment

Fig. 4. Morphologic changes of WEHI-164 cancerous cells; (A) without treatment, (B) treated by samarcandin (10 μM & 10 h). *The black arrows exhibit the dead cancerous cells.

curcumin, as a positive control, shows the less cytotoxic effect than samarcandin [34]. This anti-cancer effect at 0–200 μM concentrations was detected in a time- and dose-dependent manner. Also, the results revealed that the IC_{50} values for samarcandin were significantly different from normal fibroblasts (120 μM). Meanwhile, the morphology of cells treated with samarcandin has been altered compared to the cells without any treatment (data not shown), see Fig. 4. Microscopic data demonstrated represented that treating cells with samarcandin causes abnormal morphological changes like shrinkage in a time-dependent manner that lead to cellular vesicles and finally ends in cell death. Our data are in concordance with other similar reports showing the anti-cancer properties of cyclic sesquiterpene-coumarins. According to recent studies fesselol, isolated from *F. gumosa*, illustrated potent antiproliferative activity. It inhibited proliferation of leukemic cells (U937) with IC_{50} value of 8 μM [17]. Rassouli et al. reported that the mogoltacin existed in extract of *F. Badrakema* root showed more potent cytotoxic activity without any toxic effects on normal cells than vincristine [18]. In another study, the extract of *F. tunetana* root contained several sesquiterpene coumarins – coladonin and

isosamarcandin –, which showed weak cytotoxic activity against HTC 116 and HT-29 cell lines [19]. Thus, the purified samarcandin is the most promising candidate for further *in vitro* and *in vivo* studies.

4. Conclusion remarks

In summary, on account of increasing cancerous diseases, the experts are clearly trying to find chemicals from herbal resources. The chemical structure of samarcandin is based on a sesquiterpene moiety linked through a linkage with the 7-hydroxy group of umbelliferone skeleton. *Samarcandin* was isolated from *F. assafoetida* and characterized by FT-IR, UV, and NMR spectroscopies. In addition, the absolute atomic structure of samarcandin was confirmed by single-crystal X-ray structure analysis. The optimized molecular geometry and theoretical analysis with B3LYP and B3PW91 basis sets of samarcandin make closely an agreement to that obtained from the single crystal X-ray crystallography. Through the calculations of the first ionization potentials, HOMO, LUMO, and HOMO-LUMO gaps, it was found that samarcandin

has low energy gaps between the first ionization potentials and HOMO. It means that the low energy gap might be responsible for cytotoxic activity of samarandin. Accurate theoretical calculations can help identify and provide ways to obtain important chemical and physical information that cannot be easily obtained by experimental approaches. Furthermore, cellular toxicity was evaluated by the MTT assay on cancerous AGS and WEHI-164 cell lines. In conclusion, *In vitro* significant toxic effects as well as a noticeable morphologic changes was observed by samarandin treatment.

Acknowledgments

The authors are grateful to University of Tabriz and Golestan University (GU) for partial support of this research. The crystallography was supported 15-12653S of the Czech Science Foundation using instruments of the ASTRA lab established within the Operation program Prague Competitiveness, CZ.2.16/3.1.00/24510.

References

- [1] M. Iranshahi, M. Iranshahi, J. Ethnopharmacol. 134 (2011) 1–10.
- [2] W.C. Evans, Volatile oils and Resins, 15th ed., Trease and Evans Pharmacognosy, London, 2002.
- [3] A. Zargari, Medicinal Plants, 6th ed., Tehran University Publications, Iran, 1996.
- [4] G. Takeoka, Volatile constituents of *Assa-foetida*, in: Aroma Active Compounds in Foods, American Chemical Society, Washington, DC, 2001.
- [5] C.L. Lee, L.C. Chiang, L.H. Cheng, C.C. Liaw, A. El-Razek, H. Mohamed, F.R. Chang, Y.C. Wu, J. Nat. Prod. 72 (2009) 1568–1572.
- [6] A.A. Dehpour, M.A. Ebrahimzadeh, N.S. Fazel, N.S. Mohammed, Grasas Aceites 60 (2009) 405–412.
- [7] M. Sayyah, A. Mandgary, M. Kamalinejad, J. Ethnopharmacol. 82 (2002) 105–109.
- [8] F. Eftekhar, M. Yousefzadi, K. Borhani, Fitoterapia 75 (2004) 758–759.
- [9] R. Singh, Ind. J. Anim. Sci. 77 (2007) 675–677.
- [10] U. Sitara, I. Niaz, J. Naseem, N. Sultana, Pak. J. Bot. 40 (2008) 409–414.
- [11] P. Angelini, R. Pagiotti, R. Venanzoni, B. Granetti, Allelopathy J. 33 (2009) 357–368.
- [12] K. Aruna, V.M. Sivaramkrishnan, Food Chem. Toxicol. 30 (1992) 953–956.
- [13] M. Saleem, A. Alam, S. Sultana, Life Sci. 68 (2001) 1913–1921.
- [14] A.S. Abu-Zaiton, Pak. J. Biolog. Sci. 13 (2010) 97–100.
- [15] M. Fatehi, F. Farifteh, Z. Fatehi-Hassanabad, J. Ethnopharmacol. 91 (2004) 321–324.
- [16] P. Kumar, D.K. Singh, Chemosphere 63 (2006) 1568–1574.
- [17] M. Iranshahi, M. Masullo, A. Asili, A. Hamedzadeh, B. Jahanbin, M. Fetsa, A. Capasso, S. Piacente, J. Nat. Prod. 73 (2010) 1958–1962.
- [18] A. Jabrane, H.B. Jannet, Z. Mighri, J.-F. Mirjolet, O. Duchamp, F. Harzallah-Skhiri, M.-A. Laccaille-Dubois, Chem. Biodivers. 7 (2010) 392–399.
- [19] F.B. Rassouli, M.M. Matin, M. Iranshahi, A.R. Bahrami, V. Neshati, S. Mollazadeh, Z. Neshati, Phytomedicine 16 (2009) 181–187.
- [20] N.P. Kir'yalov, S.D. Movchan, Chem. Nat. Compd. 4 (1968) 73–77.
- [21] N.P. Kir'yalov, T.V. Bukreeva, Chem. Nat. Compd. 6 (1972) 798–799.
- [22] S.M. Nasirov, A.I. Saidkhodzhaev, T.Kh. Khasanov, M.R. Yagudaev, V.M. Malikov, Chem. Nat. Compd. 21 (1985) 171–177.
- [23] D. Troya, R.Z. Pascual, G.C. Schatz, J. Phys. Chem. A 107 (2013) 10497–10506.
- [24] S. Hafez Ghoran, S. Saeidnia, E. Babaei, F. Kiuchi, M. Dusek, V. Eigner, A. Dehno Khalaji, A. Soltani, P. Ebrahimi, H. Mighani, Bioorg. Chem. 57 (2014) 51–56.
- [25] K. Sung, F.L. Chen, Org. Lett. 5 (2003) 889–891.
- [26] Q.A. Qiao, Z.T. Cai, D.C. Feng, Y.S. Jiang, Biophys. Chem. 110 (2004) 259–266.
- [27] C.C. Su, L.H. Lu, J. Mol. Struct. 702 (2004) 23–31.
- [28] M.J. Frisch, G.W. Trucks, H.B. Schegel, G.E. Scuseria, M.A. Robb, J.R. Cheeseman, J.A. Montgomery Jr, T. Vreven, K.N. Kudin, J.C. Burant, J.M. Millam, S.S. Iyengar, J. Tomasi, V. Barone, B. Mennucci, M. Cossi, G. Scalmani, N. Rega, G.A. Petersson, H. Nakatsuji, M. Hada, M. Ehara, K. Toyota, R. Fukuda, J. Hasegawa, M. Ishida, T. Nakajima, Y. Honda, O. Kitao, H. Nakai, M. Klene, X. Li, E. Knox, H.P. Jhratchian, J.B. Cross, V. Bakken, C. Adamo, J. Jaramillo, R. Gomperts, R.E. Stratmann, O. Yazyev, A.J. Austin, R. Cammi, C. Pomelli, J.W. Ochterski, P.Y. Ayala, K. Morokuma, G.A. Voth, P. Salvador, J.J. Dannenberg, V.G. Zakrzewski, S. Dapprich, A.D. Daniels, M.C. Strain, O. Farkas, D.K. Malick, A.D. Rabuck, K. Raghavachari, J.B. Foresman, J.V. Ortiz, Q. Cui, A.G. Baboul, S. Clifford, J. Cioslowski, B.B. Stefanov, G. Liu, A. Liashenko, P. Piskorz, I. Komaromi, R.L. Martin, D.J. Fox, T. Keith, M.A. Al-Laham, C.Y. Peng, A. Nanayakkara, M. Challacombe, P.M.W. Gill, B. Johnson, W. Chen, M.W. Wong, C. Gonzalez, J.A. Pople, Gaussian 98 (Revision D.01), Gaussian Inc, Wallingford, CT, 1998.
- [29] L. Palatinus, G. Chapuis, J. Appl. Cryst. 40 (2007) 786–790.
- [30] V. Petricek, M. Dusek, L. Palatinus, Z. Kristallogr. 229 (2014) 345–352.
- [31] D.M. Suresh, M. Amalanathan, S. Sebastian, D. Sajan, I. Hubert Joe, V. Bena Jothy, Spectrochim. Acta A 98 (2012) 413–422.
- [32] Z. Bolboli Nojini, F. Yavari, S. Bagherifar, J. Mol. Liq. 166 (2012) 53–61.
- [33] L. karami, H. Behzadi, N.L. Hadipour, M. Mousavi-khoshdel, Comput. Theo. Chem. 965 (2011) 137–145.
- [34] A. Soltani, M.T. Baei, E. Tazikeh Lemeski, M. Shahini, Superlattices Microstruct. 76 (2014) 315–325.
- [35] S. Sebastian, S. Sylvestre, N. Sundaraganesan, M. Amalanathan, S. Ayyapan, K. Oudayakumara, B. Karthikeyan, Spectrochim. Acta A 107 (2013) 167–178.
- [36] L.T. Sein Jr., J. Mol. Struct. 1022 (2012) 181–188.
- [37] E. Babaei, M. Sadeghizadeh, Z.M. Hassan, M.A. Feizi, F. Najafi, S.M. Hashemi, Int. Immunopharmacol. 12 (2012) 226–234.
- [38] S. Hafez Ghoran, S. Saeidnia, E. Babaei, F. Kiuchi, H. Hussain, Nat. Prod. Res. (2015), <http://dx.doi.org/10.1080/14786419.2015.1054286>.
- [39] J. Asghari, V. Atabaki, E. Baher, M. Mazaheritehrani, Nat. Prod. Res. (2015), <http://dx.doi.org/10.1080/14786419.2015.1050669>.
- [40] A. El-Razek, H. Mohamed, O. Shinji, A.A. Ahmed, T. Hirata, Phytochemistry 58 (2001) 1289–1295.
- [41] G.F. Sousa, L.P. Duarte, A.F.C. Alcântara, G.D.F. Silva, S.A. Vieira-Filho, R.R. Silva, D.M. Oliveira, J.A. Takahashi, Molecules 17 (2012) 13439–13456.
- [42] A. Soltani, M. Bezi Javan, RSC (2015), <http://dx.doi.org/10.1039/C5RA12571E>.
- [43] A. Soltani, A. Sousaraei, M. Mirarab, H. Balakheyli, J. Saudi Chem. Soc. (2015), <http://dx.doi.org/10.1016/j.jscs.2015.06.006>.